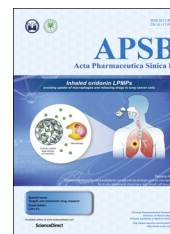




Chinese Pharmaceutical Association  
Institute of Materia Medica, Chinese Academy of Medical Sciences

Acta Pharmaceutica Sinica B

[www.elsevier.com/locate/apsb](http://www.elsevier.com/locate/apsb)  
[www.sciencedirect.com](http://www.sciencedirect.com)



ORIGINAL ARTICLE

# Inhalable oridonin-loaded poly(lactic-co-glycolic) acid large porous microparticles for *in situ* treatment of primary non-small cell lung cancer



Lifei Zhu<sup>a,b,c,†</sup>, Miao Li<sup>a,†</sup>, Xiaoyan Liu<sup>a</sup>, Lina Du<sup>a</sup>, Yiguang Jin<sup>a,b,\*</sup>

<sup>a</sup>Department of Pharmaceutical Sciences, Beijing Institute of Radiation Medicine, Beijing 100850, China

<sup>b</sup>Anhui Medical University, Hefei 230001, China

<sup>c</sup>Department of Pharmacy, Yangpu Hospital, Tongji University School of Medicine, Shanghai 200090, China

Received 3 June 2016; revised 16 August 2016; accepted 23 August 2016

## KEY WORDS

Large porous microparticle;  
Non-small cell lung cancer;  
Oridonin;  
Poly(lactic-co-glycolic) acid;  
Pulmonary delivery

**Abstract** Non-small cell lung cancer (NSCLC) accounts for about 85% of all lung cancers. Traditional chemotherapy for this disease leads to serious side effects. Here we prepared an inhalable oridonin-loaded poly(lactic-co-glycolic)acid (PLGA) large porous microparticle (LPMP) for *in situ* treatment of NSCLC with the emulsion/solvent evaporation/freeze-drying method. The LPMPs were smooth spheres with many internal pores. Despite a geometric diameter of  $\sim 10 \mu\text{m}$ , the aerodynamic diameter of the spheres was only  $2.72 \mu\text{m}$ , leading to highly efficient lung deposition. *In vitro* studies showed that most of oridonin was released after 1 h, whereas the alveolar macrophage uptake of LPMPs occurred after 8 h, so that most of oridonin would enter the surroundings without undergoing phagocytosis. Rat primary NSCLC models were built and administered with saline, oridonin powder, gemcitabine, and oridonin-loaded LPMPs *via* airway, respectively. The LPMPs showed strong anticancer effects. Oridonin showed strong angiogenesis inhibition and apoptosis. Relevant mechanisms are thought to include oridonin-induced mitochondrial dysfunction accompanied by low mitochondrial membrane potentials, downregulation of BCL-2 expressions, upregulation of expressions of BAX, caspase-3 and caspase-9. The oridonin-loaded PLGA

**Abbreviations:** BSA, bovine serum albumin; DAB, 3,3'-diaminobenzidine; DAPI, 4',6-diamidino-2-phenylindole; DPI, dry powder inhalation; EGFR, epidermal growth factor receptor; FPF, fine particle fraction; HPLC, high performance liquid chromatography; HRP, horseradish peroxidase; LPMP, large porous microparticle; NSCLC, non-small cell lung cancer; PLGA, poly(lactic-co-glycolic)acid; PVA, polyvinyl alcohol; qPCR, quantitative polymerase chain reaction; SEM, scanning electron microscopy; SLF, simulated lung fluid; TCM, traditional Chinese medicine; XRD, X-ray diffraction

\*Corresponding author. Tel.: +86 10 88215159; fax: +86 10 68214653.

E-mail address: [jinyg@bmi.ac.cn](mailto:jinyg@bmi.ac.cn) (Yiguang Jin).

<sup>†</sup>These authors made equal contributions to this work.

Peer review under responsibility of Institute of Materia Medica, Chinese Academy of Medical Sciences and Chinese Pharmaceutical Association.

<http://dx.doi.org/10.1016/j.apsb.2016.09.006>

2211-3835 © 2017 Chinese Pharmaceutical Association and Institute of Materia Medica, Chinese Academy of Medical Sciences. Production and hosting by Elsevier B.V. This is an open access article under the CC BY-NC-ND license (<http://creativecommons.org/licenses/by-nc-nd/4.0/>).

LPMPs showed high anti-NSCLC effects after pulmonary delivery. In conclusion, LPMPs are promising dry powder inhalations for *in situ* treatment of lung cancer.

© 2017 Chinese Pharmaceutical Association and Institute of Materia Medica, Chinese Academy of Medical Sciences. Production and hosting by Elsevier B.V. This is an open access article under the CC BY-NC-ND license (<http://creativecommons.org/licenses/by-nc-nd/4.0/>).

## 1. Introduction

Lung cancer is a tumor with high mortality, is responsible for 23% of all cancer-related deaths, and poses a serious threat to human health. Lung cancer may be induced by sensitive gene mutations and/or environmental changes that include cigarette smoking, air pollution, and ionizing radiation<sup>1</sup>. Rapid industrialization of many developing countries is likely to lead to heavy air pollution which causes the incidence of lung cancer to increase faster than that of other malignant tumors<sup>2,3</sup>. Lung cancer is divided into two categories: small cell lung cancer and non-small cell lung cancer (NSCLC). NSCLC, accounting for about 80%–85% of all lung cancers, is readily transferred to other parts of the body and relatively poor in prognosis (approximately 85% mortality within 5 years)<sup>4</sup>. Moreover, the lung is also a major site of metastasis for other cancers including those of the breast, prostate, and colon<sup>5</sup>.

Gemcitabine, a nucleoside analogue of deoxycytidine, is the general treatment for non-small cell lung cancer. Gemcitabine requires intracellular phosphorylation mediated by deoxycytidine kinases (dCKs) to get converted into its triphosphate form (dFdC-TP). This metabolite exerts its cytotoxic effects by incorporation into DNA and inhibiting DNA synthesis<sup>6</sup>. Systemically administered drugs (the oral or injection routes) can produce serious toxic side effects with widespread damage due *in vivo* distribution<sup>7</sup>, yet result in limited drug distribution into lung tissue<sup>8</sup>. Therefore, lung tumor-targeted drug delivery systems have become increasingly popular research topics despite the fact that they are only administered *via* intravenous injection and applied to the lung metastatic models, not primary NSCLC<sup>9,10</sup>.

Pulmonary delivery of drugs is a non-invasive method for treatment of lung diseases, in which aerosols or dry powder inhalations (DPIs) are the common dosage forms<sup>11,12</sup>. In this way, the dose in the lung can be maximized because the lung tissue is directly exposed to the aerosols or dry powders delivered *via* the airways. Additionally, the delivery is non-invasive, and thus improves patient compliance *versus* intravenous injection<sup>13</sup>. It should be an ideal chemotherapeutic approach to lung cancer compared to the oral and intravenous routes<sup>14</sup>. So far, only a few local therapies of non-primary (transplanted or metastasis) NSCLC animal models have been reported<sup>4,15–17</sup>, and *in situ* treatment of primary NSCLC has not been reported. Thus, there is a need to search for suitable drugs with weak toxicity to treat primary NSCLC, especially drugs capable of local or topical application.

The market and research of DPIs are increasing due to high drug loads, stability, user-friendliness, and patient compliance. For DPIs, the aerodynamic diameters of particles generally range from 1 to 5  $\mu\text{m}$ <sup>18,19</sup>. In most cases, the range cannot be achieved so that some modifications are needed, such as the use of lactose as the supporter. Moreover, the particles of 1–5  $\mu\text{m}$  tend to agglomerate due to van der Waals and electrostatic forces<sup>18</sup>. Another problem is that particles less than 10  $\mu\text{m}$  are prone to phagocytosis by

alveolar macrophages<sup>20</sup>. Therefore, the diameters of inhalable particles have become a dilemma. The only solution seems to lie in a novel strategy in which a large porous microparticle (LPMP) keeps a relatively apparent large diameter but with low density and small aerodynamic diameters<sup>21,22</sup>. LPMPs have been demonstrated to exhibit such ideal lung deposition profiles<sup>23</sup>.

Oridonin is an active diterpenoid isolated from a traditional Chinese medicine (TCM) *Isodon rubescens* (*Hemsli*) *Hara* (Chinese: Dong Ling Cao) which mainly grows in the Henan and Shaanxi provinces of China. This compound has been tried as an anti-inflammatory, antibacterial, and anticancer agent. Since oridonin shows anticancer effects with little adverse reactions, it has attracted much attention from oncologists and pharmacologists<sup>24</sup>. The anticancer mechanism of oridonin may involve inhibition of NF- $\kappa$ B transferring from the cytoplasm to the nucleus in the localization of metastasis, activation of caspase-mediated apoptosis pathway, and induction of apoptosis mediated by blocking the epidermal growth factor receptor (EGFR) signaling pathway<sup>25–27</sup>. Although the effects of oridonin on different cancers have been explored, clinical utilization of this drug has been highly hindered due to poor water solubility and low bioavailability. Furthermore, little is known about the effects of oridonin on lung cancer.

Here, we present a novel LPMP loading oridonin for the direct *in situ* treatment of primary NSCLC with pulmonary delivery. The formulation and preparation methods of the microparticles were optimized and the characteristics and drug release of the microparticles were investigated. Finally, substantial anticancer effects of the microparticles were demonstrated on the rat primary NSCLC models and the relevant mechanisms were explored.

## 2. Materials and methods

### 2.1. Materials

Oridonin was obtained from the Shaanxi Huike Botanical Development Co., Ltd., Shaanxi, China. Poly(lactic-*co*-glycolic)acid (PLGA, lactide/glycolide, 50:50, mol/mol, MW 10 kDa) was produced by Jinan Daigang Biomaterial Co., Ltd., Shandong, China. Gemcitabine, used as a positive control drug, was purchased from Hansoh Pharmaceutical Co., Ltd., Jiangsu, China. Polyvinyl alcohol (PVA, 87%–89% alcoholysis, MW 75000 Da) was purchased from the Aladdin Industrial Corporation, Shanghai, China, and ammonium bicarbonate was purchased from the Sinopharm Chemical Reagent Co., Ltd., Beijing, China. Cy7 was purchased from Fanbo Biochemicals Co., Ltd., Beijing, China. 3-Methyl cholanthrene (MCA, Sigma, USA), diethyl nitrosamine (DEN, Tokyo Chemical Industry, Japan), and iodized oil (Guerbet, French) were used. Anti-BCL-2 and anti-BAX antibodies were from the Cell Signaling Technology Inc. (Danvers, USA). All other chemicals and solvents were of analytical grade or high performance liquid chromatographic (HPLC) grade.

## 2.2. Animals

Male Wistar rats (180–200 g) from the Beijing Vital River Experimental Animal Technology Co., Ltd. (Beijing, China) were used. The handling and surgical procedures related to the animals were conducted in strict accordance with the Guiding Principles for the Use of Laboratory Animals of Beijing Institute of Radiation Medicine (BIRM). The animal experiments were approved by the institute's animal subject review committee of BIRM. Lung tissues were excised after sacrifice. All efforts were made to reduce the number of animals used and to minimize animals' suffering.

## 2.3. Preparation of oridonin-loaded LPMPs

PLGA, a highly biocompatible and biodegradable copolymer, also approved by the Food and Drug Administration (FDA) of the United States of America for biomedical application, was used as the major component of LPMPs. The PLGA LPMPs were prepared with a water-in-oil-in-water (w/o/w) emulsion solvent evaporation method<sup>28,29</sup>. Ammonium bicarbonate ( $\text{NH}_4\text{HCO}_3$ ) that decomposed to ammonia and  $\text{CO}_2$  at high temperatures and low air pressures was used as the pore forming agent in the preparation of LPMPs<sup>30</sup>. Simply, oridonin (80 mg) and PLGA (700 mg) were dissolved in methylene chloride (2 mL), and then mixed with a  $\text{NH}_4\text{HCO}_3$  solution (1.5%, 0.4 mL). A 70-W probe-type sonicator was used to make the w/o emulsions that were mixed with a PVA solution (1%, 25 mL) and then homogenized for preparation of w/o/w emulsions. Organic solvents were removed from the emulsions after stirring overnight. Solid micro-particles were collected after high-speed centrifugation, washed with water, and lyophilized (Supplementary materials, Fig. S1). The Cy7-loaded PLGA LPMPs and the Cy7-loaded or oridonin-loaded conventional intact PLGA microparticles without  $\text{NH}_4\text{HCO}_3$  were also prepared according to the above procedure.

## 2.4. In vitro release study

The oridonin-loaded PLGA LPMPs (50 mg) were poured in a triangular flask and suspended in 50 mL of the simulated lung fluid (SLF) containing 0.02% Tween 80. The flask was placed on a shaker (160 rpm, THZ-D, Taicang laboratory factory, China) at  $37 \pm 0.5$  °C. At the predetermined time intervals, the sample (1 mL) was withdrawn and centrifuged at 5000 rpm for 10 min (TGL-16B, Shanghai Anting scientific instrument factory, China). The supernatant was filtered through a 0.45- $\mu\text{m}$  filter and analyzed with the HPLC. The fresh SLF of an equal volume was supplemented to the flask. The experiments were performed in triplicates. Additionally, the surface morphologies of the microparticles at different time points were investigated with SEM.

## 2.5. In vivo lung deposition study

In the *in vivo* deposition experiments, the Cy7-loaded PLGA LPMPs were quickly administered to the rat lung using an insufflator (DP-4M, Penn-Century Inc., PA, USA) through the trachea without anesthesia. To confirm the lung deposition of microparticles, the tissue sections and the whole lung were observed using fluorescence microscopy and the imaging station (IVIS Spectrum CT, Perkin Elmer, US), respectively. The non-large porous PLGA microparticles were used as a control to compare the lung deposition efficiency of the LPMPs.

## 2.6. Pharmacodynamic study

We established the primary NSCLC rat model using the chemical induction of pulmonary delivered MCA and DEN referred to the literature<sup>31</sup>, though pharmacotherapy had not been performed by others on this primary lung cancer model. However, the primary model highly resembled the clinical NSCLC compared to other lung cancer models.

Healthy rats were divided into 4 groups of 6 each. The iodized oil (0.15 mL) containing 100 mg MCA/mL and 10% DEN as the carcinogen was sprayed into the left lobes of rat lungs using the soft long plastic tubes linked to a 1-mL syringe pre-filled with the solution. Development of the primary NSCLC model took 30 days.

Lung cancer rats were administered saline (0.2 mL per rat) *via* airways using an intratracheal aerosolizer (IA-1B, Penn-Century Inc., PA, USA) once a week for 4 weeks. The raw oridonin powder (1 mg each rat) and the oridonin-loaded PLGA LPMPs (10 mg each rat, containing 1 mg of oridonin) were sprayed into the lung cancer rats using an insufflator (DP-4M, Penn-Century Inc., PA, USA) through trachea without anesthesia once a week for 4 weeks. A gemcitabine (10 mg/mL) solution in 0.9% NaCl solutions was also sprayed into the lung cancer rat lungs using the intratracheal aerosolizer at the dose of 0.1 mL each rat once a week for 4 weeks. The rats were sacrificed after treatment for 31 days, *i.e.*, after 3 days following 4 times of administrations. The whole lung was observed with the imaging station as mentioned above. The left lung was split into two parts. One was rapidly frozen in liquid nitrogen and kept at  $-80$  °C for biological measurement. The other was fixed after being immersed in the 4% paraformaldehyde solution followed by histopathological evaluation.

All of the lung cancer rats were injected through the trachea without anesthesia. The solutions and the powders were delivered using an intratracheal aerosolizer (IA-1B, Penn-Century Inc., PA, USA) and an insufflator (DP-4M, Penn-Century Inc., PA, USA), respectively. The rats in the four groups were treated with the following agents once a week for 4 weeks: (A) saline (0.2 mL per rat); (B) the raw oridonin powder (1 mg each rat); (C) a gemcitabine (10 mg/mL) solution in 0.9% NaCl solutions (0.1 mL each rat); and (D) the oridonin-loaded PLGA LPMPs (10 mg each rat, containing 1 mg of oridonin). Rats were sacrificed after treatment for 31 days, *i.e.*, 3 days later after the final administration. The whole lung was observed with the imaging station as mentioned above. The left lung was split into two parts. One was rapidly frozen in liquid nitrogen and kept at  $-80$  °C for biological measurement. The other was fixed after being immersed in the 4% paraformaldehyde solution followed by histopathological evaluation.

## 2.7. Immunohistochemistry

The sections of left lungs, initially embedded in paraffin, were deparaffinized, rehydrated, and microwave-heated for 15 min in the EDTA antigen retrieval solution (pH 8.0) for antigen retrieval. Then, a 3% hydrogen peroxide solution was applied to block the endogenous peroxidase activity. Furthermore, the sections were immersed in the bovine serum albumin (BSA) solutions for 15 min to block non-specific proteins which adhered the tissues. The primary antibody of CD31 (Goodbio, China) diluted with a 3% BSA solution was added to the above tissues and incubated overnight at 4 °C. The sections were washed with PBS for three

times and 5 min once. The secondary antibody of primary antibody was added and incubated for 30 min at room temperature followed by interval PBS washing. The sections were immersed for 5 min in the coloring substrate 3,3'-diaminobenzidine (DAB, 0.4 mg/mL, DAKO, USA) containing 0.003% hydrogen peroxide, rinsed with water, counterstained with hematoxylin, dehydrated, and cover-slipped. The sections were further observed under a microscope.

### 2.8. Apoptosis assay of lung tissues

The left lungs were fixed in the 4% paraformaldehyde solution, and embedded in paraffin. To assay cellular apoptosis, the terminal deoxynucleotidyl transferase biotin-dUTP nick end labeling (TUNEL, Roche, Switzerland) staining was performed and incubated for 1 h at 37 °C. After PBS washing, the sections were incubated with DAPI (4',6-diamidino-2-phenylindole) for 10 min at room temperature to detect nucleoli. Images of tunel and DAPI fluorescence were recorded using a fluorescent microscope.

### 2.9. Western blot analysis of BCL-2 and BAX expressions

Proteins in the lung tissues were extracted in the Rapa buffer at 4 °C for 30 min. After centrifugation at  $13,000 \times g$  for 10 min, quantification of proteins was performed using a BCA kit (CWBI, China). The proteins were then separated with SDS-PAGE and electrophoretically transferred onto polyvinylidene fluoride membranes (Millipore, USA). The membrane was blocked with 5% non-fat milk for 1 h at room temperature, and then incubated with the indicated primary antibody overnight at 4 °C and subsequently with the horseradish peroxidase (HRP)-coupled secondary antibody. The immunoblots were reprobed with an anti- $\beta$ -actin antibody as a loading control. The protein intensity was quantified using the

ImageJ software (the National Institutes of Health, US) and normalized to the intensity of loading control  $\beta$ -actin.

### 2.10. Flow cytometry

Flow cytometry for expressions of mitochondrial membrane potentials (MMPs) was done using a BD Biosciences FACS machine (BD Immunocytometry Systems, USA) with the standard technique. The mitochondria were harvested from the fresh rat lung cancer tissues using the tissue mitochondrial isolation kit (Beyotime, China). A cationic dye, JC-1 (Beyotime, China), was used to monitor the MMPs. The fluorescence intensity was monitored using the flow cytometric instrument at the maximal excitation/emission wavelengths of 525/590 nm.

### 2.11. qPCR analysis of caspase-3 and caspase-9 levels

Total RNA was isolated from the rat lung cancer tissues using the trizol reagent (Invitrogen Life Technologies, US) according to the manufacturer's instructions, and quantified at 260 nm. The RNA purity was assessed with the ratio of optical density (OD) at 260/280 nm. The integrity was evaluated with electrophoresis on the 1% agarose gels. The cDNA was synthesized from 2  $\mu$ g of total RNA using the Revert Aid First Strand cDNA Synthesis Kit (Thermo, Germany). The primer sequences used in this study were as follows: caspase-3 forward 5'-GAAAGCCGAAACTCTTCATCAT-3'; caspase-3 reverse 5'-ATGCCATATCATCGTCAGTTC-3'; caspase-9 forward 5'-GGGACTCAAATCAAAGGAGCAGA-3'; caspase-9 reverse 5'-AGGGCAGAAGTTCACGTTGTGA-3'. All of the real-time polymerase chain reactions (qPCR) were performed with the ABI Prism 7300 sequence detection system (Applied Biosystems, Foster City,

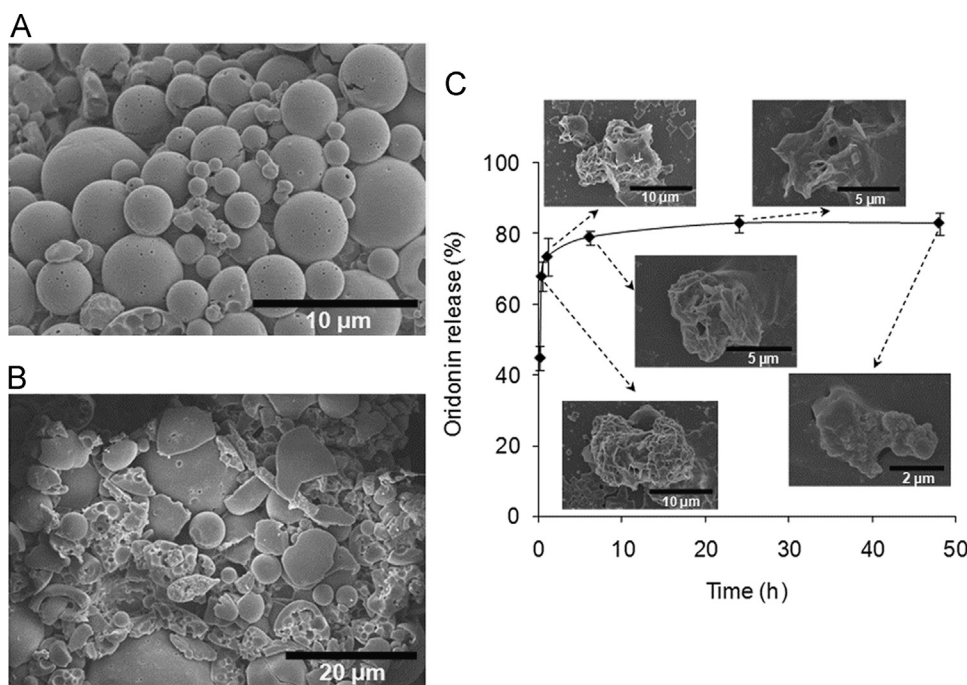


**Figure 1** SEM images of oridonin-loaded LPMPs (A) and grinded LPMPs (B), and the oridonin release profile from the PLGA LPMPs and the corresponding SEM images of microparticles (C). The LPMPs have smooth sphere surfaces with many pores on the surfaces and cavities in the inner spaces. Oridonin is rapidly released from the LPMPs and the microparticles show time-dependent erosions.

CA) and the SYBR Green I dye (Roche, Inc.). The threshold cycle numbers were obtained using the ABI Prism 7300 SDS software.

### 2.12. Statistical analysis

Student's *t*-tests were used to determine significance. All error bars represent standard deviations (SDs). Statistical significance was identified when the *P* value was  $<0.05$ .

## 3. Results and discussion

### 3.1. Optimal formulation and characteristics of oridonin-loaded LPMPs

The optimal formulation of oridonin-loaded LPMPs was prepared from 1.5% ammonium bicarbonate solution, 35% PLGA solution, and 1% PVA solution, where ammonium bicarbonate and PVA were eliminated from the final microparticles that contained  $9.3 \pm 0.1\%$  oridonin with a high encapsulation efficiency of  $81.5 \pm 1.0\%$ .

The oridonin-loaded PLGA LPMPs were smooth spheres with many small pores on the surfaces according to the scanning electron microscopic (SEM) image (Fig. 1A). Most of the LPMPs had microscale diameters of about 10  $\mu\text{m}$ . Furthermore, after artificially grinding of LPMPs, a large number of cavities were in the inner spaces (Fig. 1B). The geometric diameter of LPMPs was  $11.6 \pm 2.3 \mu\text{m}$  ( $D_{50}$ ) according to the laser light scattering method. Therefore, the LPMPs showed a very low mean tapped density of  $0.057 \pm 0.014 \text{ g/mL}$  and a small mean aerodynamic diameter of  $2.7 \pm 0.3 \mu\text{m}$ . The smooth spherical surface of LPMPs made them easily flowable with a small mean repose angle of  $26.5 \pm 4.1^\circ$ . Based on the appropriate aerodynamic diameter and good flow characteristics, the LPMPs had a high emitted dose of 71.5%, indicating that a high proportion of the LPMPs would be inhaled into the lung. Additionally, the X-ray diffraction (XRD) pattern and differential scanning calorimetric (DSC) analysis showed that oridonin adopted an amorphous form with high dispersion in the PLGA microparticle matrix (Supplementary materials, Figs. S2 and S3).

Oridonin showed a relatively rapid release from the LPMPs, with approximately 74% of the release finished after 1 h (Fig. 1C). This rapid release permitted oridonin to enter the cancer cells and achieve a sufficient accumulation in the cells before the eroded microparticles could be phagocytized by the lung macrophages.

We explored the mechanism of oridonin release from the LPMPs. The SEM images of LPMPs were made in the course of release measurements. Significant erosions of LPMPs appeared at 1 h and a number of pores were exposed (Fig. 1C), creating favorable conditions and routes for the release of drug. Furthermore, the slight water solubility (0.75 mg/mL) of oridonin<sup>32</sup>, the amorphous form, and the possibly high distribution of oridonin on the LPMP surface could improve the early rapid release of oridonin<sup>33</sup>. A Ritger-Peppas model was used to describe the release profile of oridonin from the LPMPs. The model results suggest that oridonin release was mainly due to the combination of diffusion and PLGA erosion of the PLGA LPMPs (Supplementary materials, Section 4). Comparatively, the release of oridonin from other formulations was not as good as from oridonin-loaded LPMPs, such as nanostructured lipid carriers<sup>34</sup>, solid dispersions<sup>35</sup>, or albumin nanoparticles<sup>36</sup>. Other important information obtained from the SEM images was the accelerated eroding behavior of LPMPs (Fig. 1C), resulting from the hydrolysis of PLGA and the

porous structure of LPMPs. Two days later, only a little of the microparticle residues remained, suggesting that the LPMPs did not accumulate in the lung. The rapid and complete degradation of the LPMPs suggests that the elimination of PLGA in the lung (with final products being  $\text{CO}_2$  and water) should be straightforward. Therefore, the pulmonary safety of PLGA LPMPs can be ensured.

### 3.2. Alveolar macrophage uptake of LPMPs

LPMPs are resistant to alveolar macrophage uptake, particularly before the release of loaded drugs. In the previous section, the rapid release of oridonin from the LPMPs after 1 h was introduced. We next determined if the LPMPs were phagocytized within this time frame.

We incubated Wistar rat alveolar macrophages co-incubated with the Rhodamine B-loaded LPMPs to assess the degree of phagocytosis. At time points up to 24 h, the macrophages showed various degrees of uptake of microparticles (Supplementary materials, Fig. S4). Within 8 h, no uptake was observed. At 12 h, only a little green fluorescence appeared in the macrophages and strong fluorescence appeared at 24 h. Interestingly, the uptake behavior of alveolar macrophages was closely related to the erosion processes of LPMPs. According to the SEM images of eroded LPMPs in the previous section, the size of residual LPMPs gradually decreased with time-dependent erosions, with improving macrophage uptake related to small sizes. This experiment further demonstrated that oridonin could be released and had many opportunities to enter cancer cells before alveolar macrophage uptake. There are other reports that large particles of  $\sim 10 \mu\text{m}$  have very little or no macrophage uptake, while significant uptake was reported for 4–5  $\mu\text{m}$  particles<sup>23,37</sup>. Therefore, LPMPs are suitable for pulmonary delivery of anticancer drugs.

### 3.3. *In vitro* and *in vivo* lung depositions of LPMPs

A Next Generation Impactor (NGI, Copley Scientific Limited, UK) was used to evaluate the *in vitro* distribution of inhalable microparticles to simulate lung deposition. In this study, the oridonin-loaded PLGA LPMPs were deposited in the 2–8 stages up to about 29.65% fine particle fraction (FPF), much higher than the conventional intact PLGA microparticles (only 14.28% FPF) (Supplementary materials, Fig. S5). The 2D CT imaging further showed that there was much more *in vivo* lung deposition of LPMP-loaded Cy7 than that of conventional microparticle-loaded Cy7 (Fig. 2a). More importantly, most of the LPMPs were deposited in the depth of the lung according to the 3D imaging while almost all the conventional microparticles were deposited in the upper trachea and bronchi close to the throat (Fig. 2b). These findings suggest that a low inhalation efficacy of the conventional microparticles as compared to the high lung deposition of LPMPs. Lung tissue section images validate this conclusion (Fig. 2c). This ideal lung deposition can be ascribed to the porous property and appropriate aerodynamic diameter of the presently-studied LPMPs, which are suitable for the pulmonary delivery of oridonin.

### 3.4. High anticancer efficacy of oridonin-loaded LPMPs

A large number of tumor nodes appeared in the left lungs of the saline group after 31 days administration, also shown in the CT images (Fig. 3A). The oridonin powder group showed fewer tumor nodes than

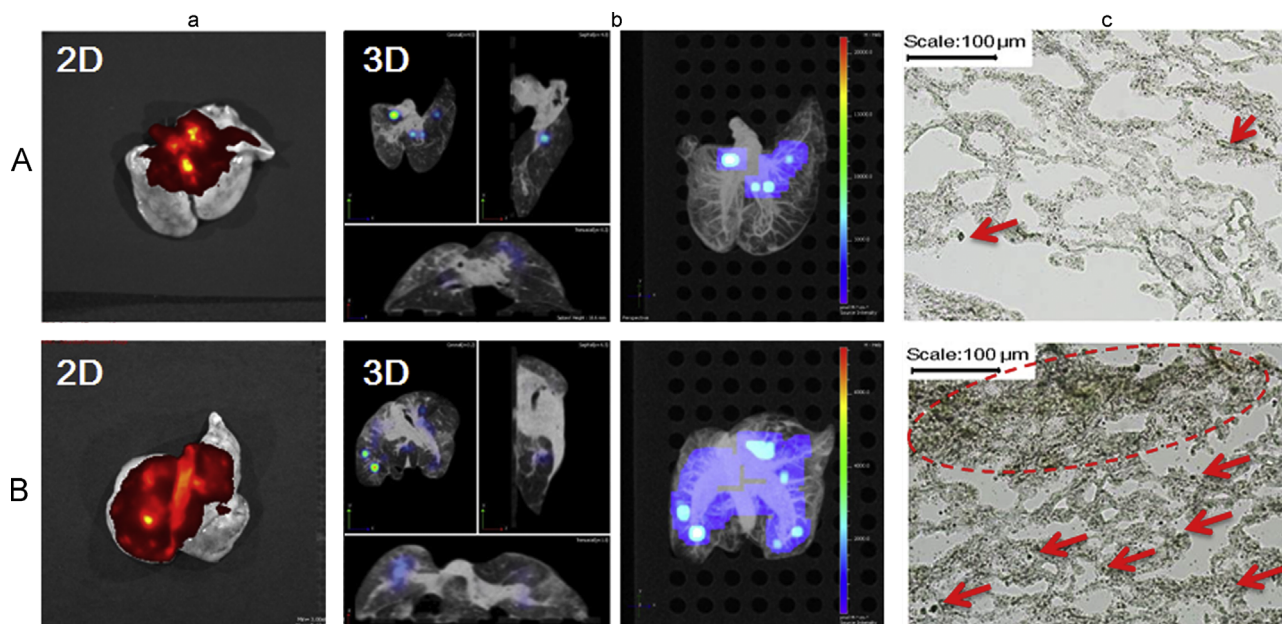


**Figure 2** Lung deposition of microparticles shown by the 2D images (a), 3D images (b), and lung tissue section images (c, 100 ×) of conventional intact Cy7-loaded PLGA microparticles (A) and Cy7-loaded PLGA LPMPs (B) after pulmonary administration to the rats for 2 h. The arrows and circle in the images (c) show the deposited microparticles in lung tissues.

the saline group (Fig. 3B). Surprisingly, the oridonin-loaded LPMP group showed only a very few nodes (Fig. 3D), similar to findings from the gemcitabine group. Therefore, the oridonin-loaded LPMPs had almost the same therapeutic efficacy as the first-line anticancer drug gemcitabine. Compared to oridonin powders without formulations, the much higher anticancer efficacy of the oridonin-loaded LPMPs demonstrated the key role of LPMP formulations for the treatment of primary NSCLC due to their high lung deposition, rapid release, and weak elimination. Moreover, the oridonin-loaded LPMPs play a more important role for the treatment of lung cancer than the other groups, which was studied and described in depth in the following sections.

### 3.5. Inhibition of angiogenesis induced by oridonin

Tumor growth and metastasis require sufficient nutrients and oxygen *via* angiogenesis<sup>38</sup>. CD31, a membrane protein constitutively expressed on the surface of endothelial cells of blood vessels, can determine the growth potential of cancer. In our experiment, the saline group showed a high degree of CD31 expression (Fig. 4A), whereas the oridonin powder and gemcitabine groups showed some CD31 expression (Fig. 4B and 4C). However, the oridonin-loaded LPMP group showed almost no CD expression. These results suggest that the anti-angiogenesis effect of oridonin may be one of anti-NSCLC mechanisms.

### 3.6. Apoptosis of lung cancer cells induced by oridonin

Apoptosis is a key mechanism by which chemotherapeutic agents induce cytotoxic effects in cancer cells<sup>39</sup>. In this study, the apoptosis of NSCLC cells was shown after merging DAPI staining and tunel staining (Fig. 5). The saline group had no apoptosis (Fig. 5A), the oridonin powder group showed a little apoptosis (Fig. 5B), and the gemcitabine group showed more apoptosis than the oridonin powder group (Fig. 5C). Furthermore, the oridonin-loaded LPMP group showed the highest apoptosis among these groups (Fig. 5D),

suggesting the high NSCLC cellular apoptosis effect of oridonin improved by the inhalable LPMP formulation. The pathological sections also exhibited similar histological results to the apoptosis (Fig. 5), wherein the oridonin-loaded LPMPs could attenuate cell proliferation in the pulmonary alveoli and small bronchus compared to the other groups.

### 3.7. Mitochondrial dysfunction induced by oridonin

Mitochondrial dysfunction causes apoptosis<sup>40</sup>. MMPs are usually used to evaluate mitochondrial dysfunction, where high MMPs indicate weak mitochondrial dysfunction or *vice versa*<sup>41</sup>. In this study, a red fluorescent marker, JC-1 was used to evaluate MMPs. Strong red fluorescence appeared when JC-1 was integrated with complete mitochondrial membranes<sup>42</sup>. However, green fluorescence appeared when JC-1 escaped from the destroyed mitochondria with low MMPs. The saline group showed strong red fluorescence, *i.e.*, high MMPs (Fig. 6A), suggesting the presence of complete mitochondria in the NSCLC cells. However, the other groups showed strong green fluorescence, *i.e.*, low MMPs, suggesting that they had anti-NSCLC effects. Moreover, the MMPs of the oridonin-loaded LPMP group were significantly lower than those of the oridonin powder group ( $P < 0.05$ ), and were not different from the gemcitabine group. Therefore, the inhalable LPMP formulation improved the mitochondrial dysfunction effect of oridonin and the subsequent apoptosis.

### 3.8. Oridonin downregulates BCL-2 expression and upregulates BAX expression

BCL-2 is an anti-apoptotic factor that prevents the release of cytochrome *c*, whereas BAX participates in the release of cytochrome *c* by translocation to the mitochondria in response to apoptotic stimuli<sup>43</sup>. We used Western blot analysis to evaluate the expressions of BCL-2 and BAX in the lysates of NSCLC tissues. The oridonin-loaded LPMP group showed the higher BAX and the

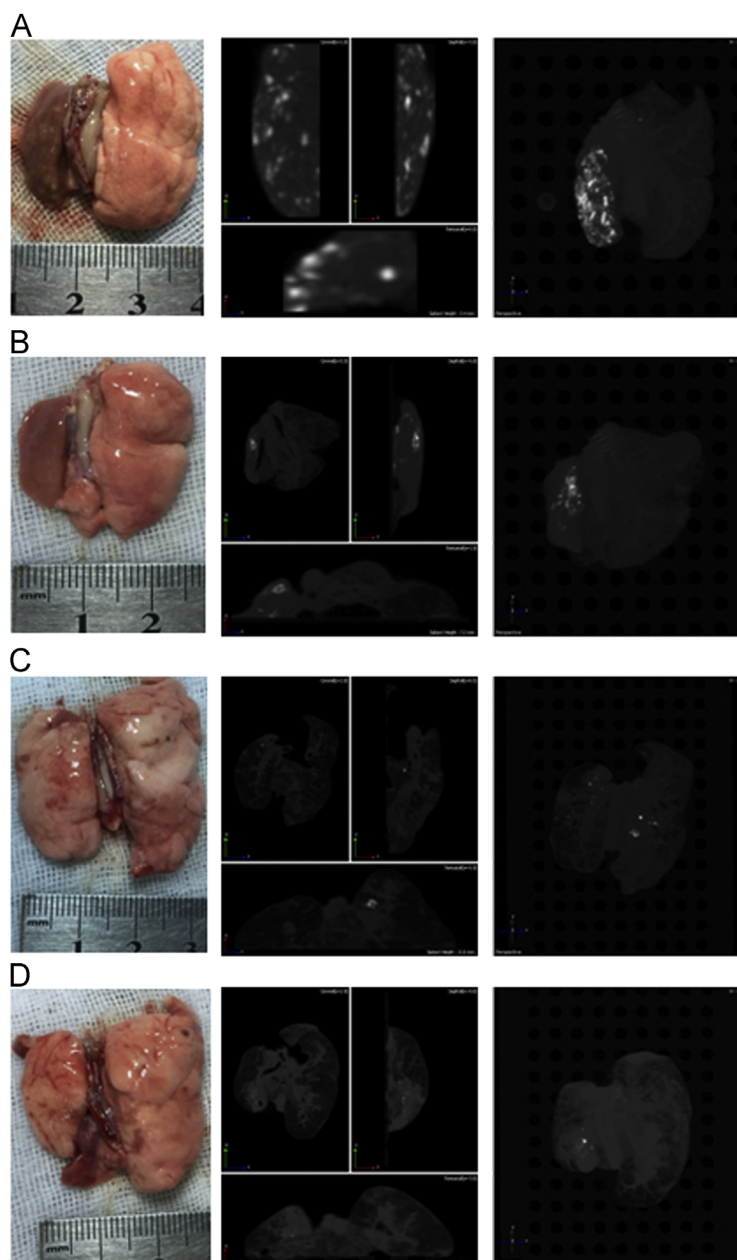


**Figure 3** Lung appearances and CT images of the lung cancer rats treated with saline (A), oridonin powders (B), gemcitabine (C), and oridonin-loaded LPMPs (D) after pulmonary delivery. The light points indicate the tumor nodes shown in the CT images.

lowest BCL-2 expressions among these groups with statistical significances (Fig. 6B), suggesting that the LPMP formulation improved the intrinsic apoptotic pathway of oridonin.

### 3.9. Gene expressions of caspase-3 and caspase-9 are improved by oridonin

Activation of the caspase pathway leads to apoptosis in the progress of cancers, where caspase-9 and caspase-3 were activated in turn<sup>44</sup>. We used qPCR to determine the levels of caspase-3 and caspase-9 in lung cancer tissues. The oridonin-loaded LPMP group showed the highest caspase-3 level but its caspase-9 level was lower than that of the gemcitabine group (Fig. 6C). We hypothesize that oridonin could improve caspase-3 activation in other ways besides caspase-9 activation. However, gemcitabine has a unique caspase-9 to

caspase-3 activation cascade pathway<sup>45</sup>. It is known that chemotherapeutic drugs may induce the production of resistant cancer cells after long-term therapies due to the single signal pathway<sup>46</sup>. Therefore, oridonin could have the ability to resist the production of resistant cancer cells due to its multiple mechanisms.

## 4. Conclusions

Here we report an inhalable oridonin-loaded PLGA LPMP for *in situ* treatment of the primary NSCLC-type lung cancer. The microparticles are of large porous structures and low tapping density, resulting in appropriate aerodynamic diameters, highly efficient lung deposition, and escape from phagocytosis due to the large sizes, all of which are ideal characteristics of lung-inhaled particles. The rapid release of oridonin

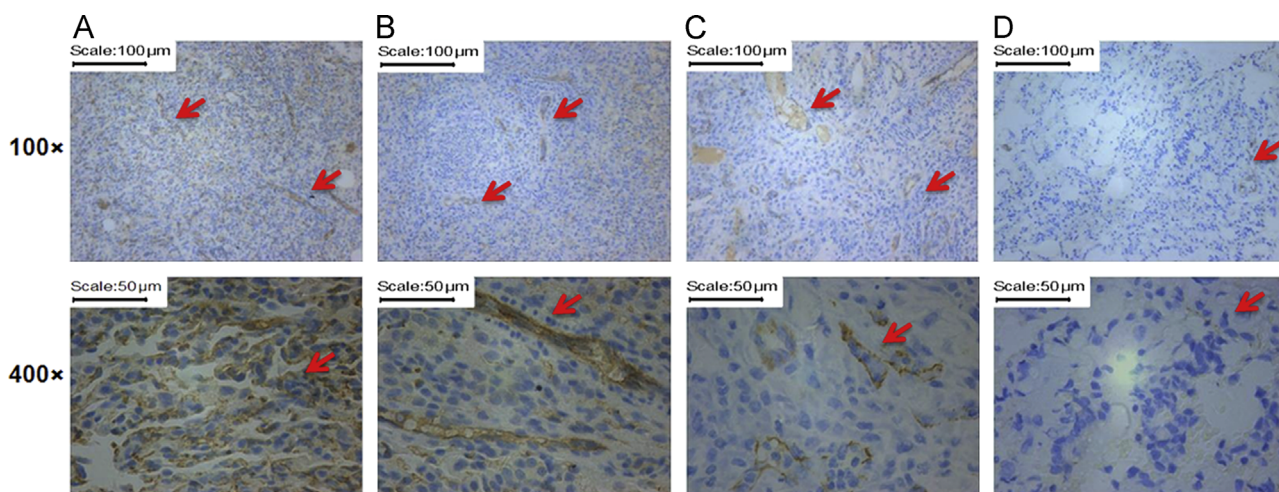


**Figure 4** CD31 expressions in the primary NSCLC tissues from rats treated with saline (A), oridonin powders (B), gemcitabine (C), and oridonin-loaded LPMPs (D) *via* pulmonary delivery. The arrows indicate the CD31 expressions shown with brown points.

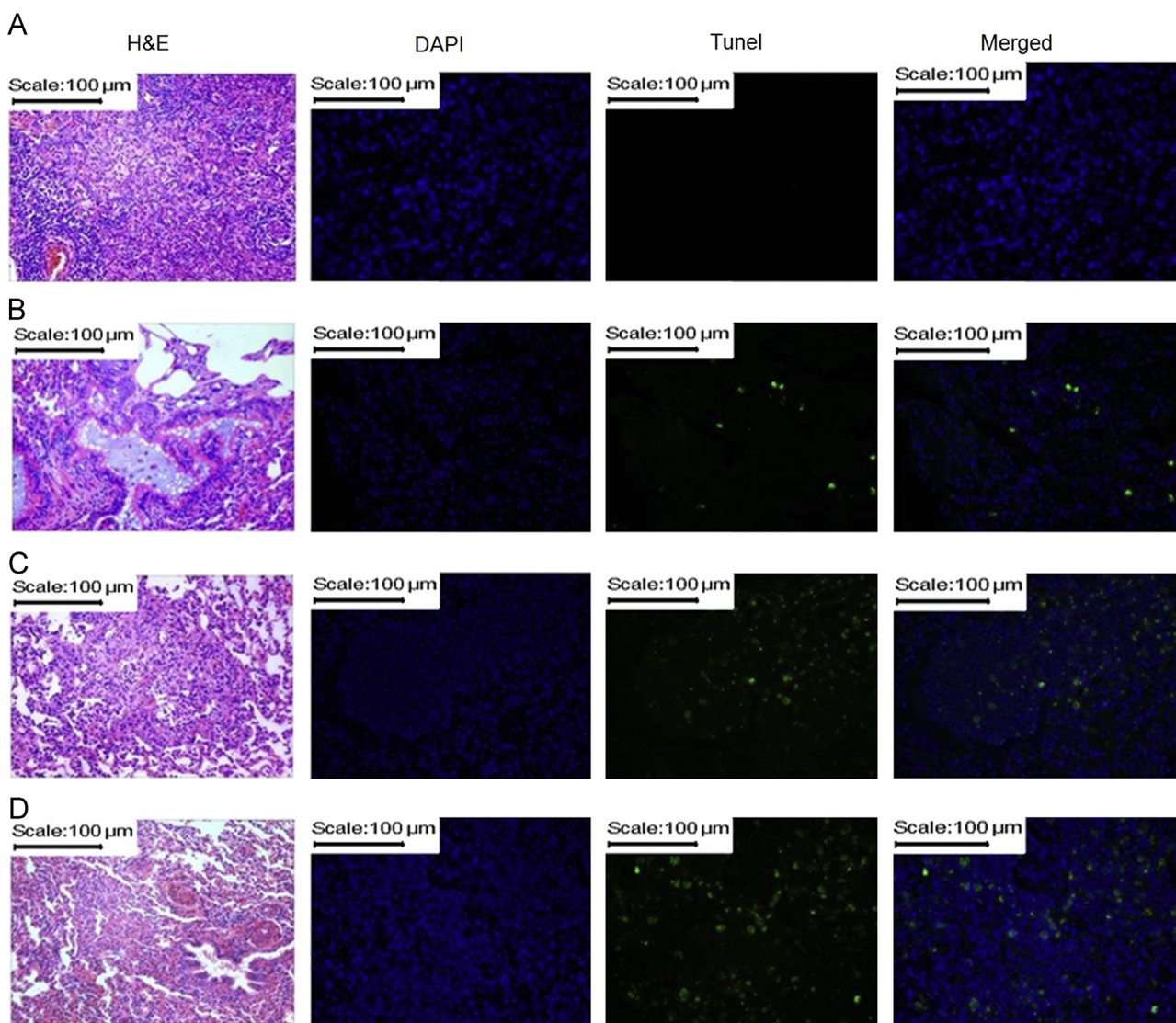


**Figure 5** Apoptosis of NSCLC cells and pathological sections of the lung tissues of rats treated with saline (A), oridonin powders (B), gemcitabine (C), and oridonin-loaded LPMPs (D) after pulmonary delivery. Apoptosis is indicated by tunnel staining (400 ×). The nuclei are shown by DAPI staining (400 ×). The merged images of tunnel and DAPI staining show the apoptosis in the NSCLC cells. Hematoxylin and eosin (H&E) staining (100 ×) shows the states of NSCLC cells.

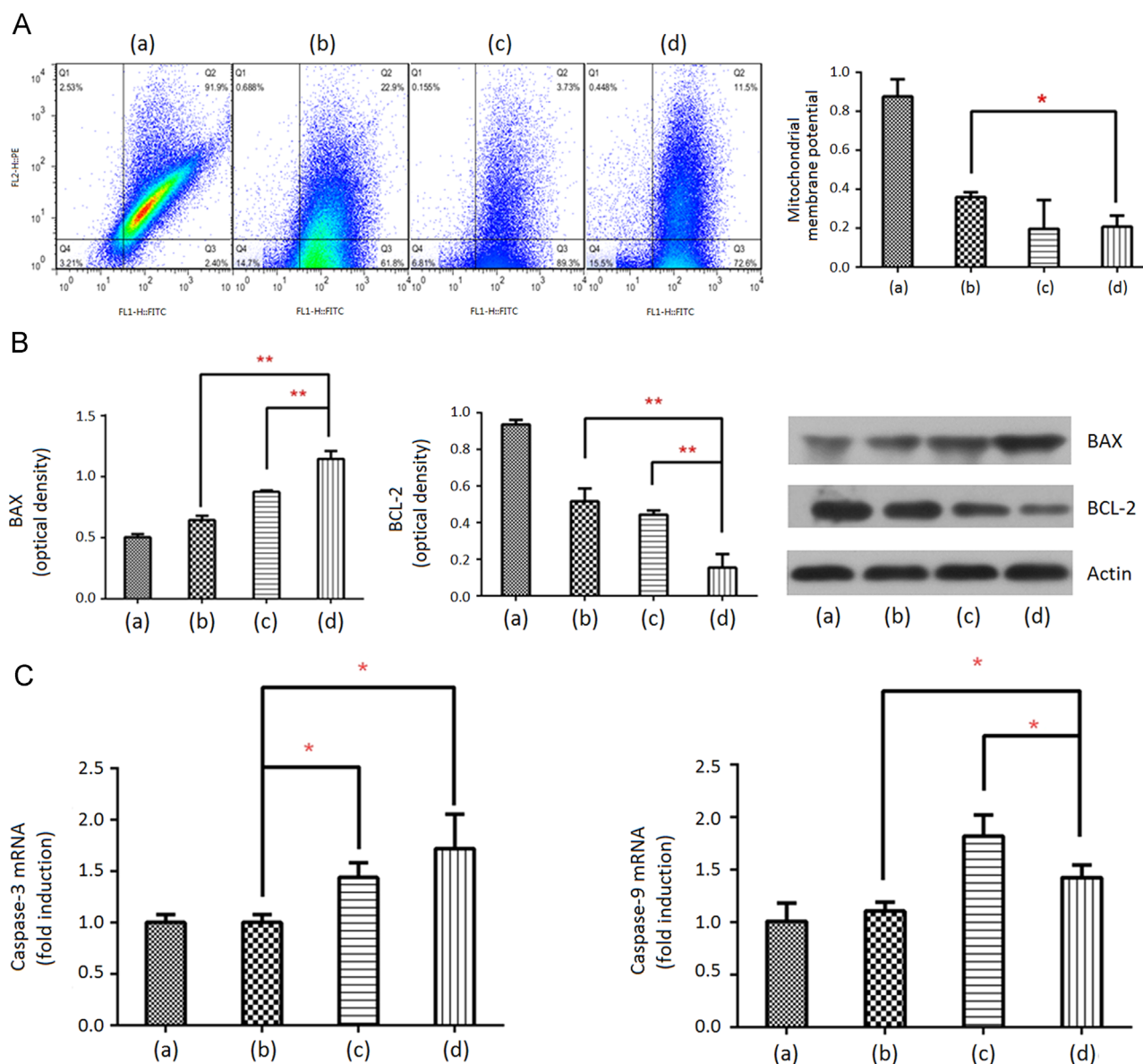


**Figure 6** Apoptosis related expressions in the NSCLC cells. Flow cytometric graphs of mitochondrial membrane potentials (MMPs) (A); regulation of pro-apoptotic protein BAX and anti-apoptotic protein BCL-2 levels (B); and stimulation of caspase-3 and caspase-9 mRNA (C) in the NSCLC cells. Columns (a), (b), (c) and (d) indicate the rats treated with inhaled saline, oridonin powders, gemcitabine and oridonin-loaded LPMPs, respectively. Q2 and Q3 area in (A) indicates high and low MMPs, respectively. Data are expressed as mean  $\pm$  SD ( $n=3$ ). \*\* $P<0.01$ ; \* $P<0.05$ .

from the LPMPs enables the drug to enter lung cancer cells before phagocytosis. More importantly, the oridonin-loaded PLGA LPMPs showed high anti-NSCLC effect due to directly action on cancer cells after pulmonary delivery. Improvement of lung cancer cell apoptosis may be a major anti-chemotherapeutic mechanism. LPMPs are promising dry powder inhalations for *in situ* treatment of lung cancer.

### Acknowledgments

The work was supported in part by grants from the National Key Technologies R&D Program for New Drugs of China (No. 2012ZX09301003-001-009) and the Beijing Natural Science Foundation of China (No. 7154230). The authors thank Prof. Xiansheng Lu for help with language editing and proof reading.

### Appendix A. Supporting information

Supplementary data associated with this article can be found in the online version at <http://dx.doi.org/10.1016/j.apsb.2016.09.006>.

### References

1. Raaschou-Nielsen O, Andersen ZJ, Beelen R, Samoli E, Stafoggia M, Weinmayr G, et al. Air pollution and lung cancer incidence in 17 european cohorts: prospective analyses from the european study of cohorts for air pollution effects (escape). *Lancet Oncol* 2013;**14**:813–22.
2. Jemal A, Bray F, Center MM, Ferlay J, Ward E, Forman D. Global cancer statistics. *CA Cancer J Clin* 2011;**61**:69–90.
3. Torre LA, Bray F, Siegel RL, Ferlay J, Lortet-Tieulent J, Jemal A. Global cancer statistics. *CA Cancer J Clin* 2015;**65**:87–109.

4. Xu C, Wang P, Zhang J, Tian H, Park K, Chen X. Pulmonary codelivery of doxorubicin and sirna by pH-sensitive nanoparticles for therapy of metastatic lung cancer. *Small* 2015;**11**:4321–33.
5. Kaminskas LM, McLeod VM, Ryan GM, Kelly BD, Haynes JM, Williamson M, et al. Pulmonary administration of a doxorubicin-conjugated dendrimer enhances drug exposure to lung metastases and improves cancer therapy. *J Control Release* 2014;**183**:18–26.
6. Jin Y, Lian Y, Du L, Wang S, Su C, Gao C. Self-assembled drug delivery systems. Part 6: *in vitro/in vivo* studies of anticancer *n*-octadecanoyl gemcitabine nanoassemblies. *Int J Pharm* 2012;**430**:276–81.
7. Cardinale D. Anthracycline-induced cardiomyopathy: clinical relevance and response to pharmacologic therapy. *J Am Coll Cardiol* 2010;**55**:213–20.
8. Rashid N, Koh HA, Baca HC, Li Z, Malecha S, Abidoye O, et al. Clinical impact of chemotherapy-related adverse events in patients with metastatic breast cancer in an integrated health care system. *J Manag Care Spec Pharm* 2015;**21**:863–71.
9. Patel AR, Chougule M, Singh M. EphA2 targeting pegylated nano-carrier drug delivery system for treatment of lung cancer. *Pharm Res* 2014;**31**:2796–809.
10. Shen H, Shi H, Xie M, Ma K, Li B, Shen S, et al. Biodegradable chitosan/alginate BSA-gel-capsules for pH-controlled loading and release of doxorubicin and treatment of pulmonary melanoma. *J Mater Chem B* 2013;**1**:3906–17.
11. Kim YK, Xing L, Chen BA, Xu F, Jiang HL, Zhang C. Aerosol delivery of programmed cell death protein 4 using polysorbitol-based gene delivery system for lung cancer therapy. *J Drug Target* 2014;**22**:829–38.
12. Gupta N, Su X, Popov B, Lee JW, Serikov V, Matthay MA. Intrapulmonary delivery of bone marrow-derived mesenchymal stem cells improves survival and attenuates endotoxin-induced acute lung injury in mice. *J Immunol* 2013;**179**:1855–63.
13. Tseng CL, Wu SY, Wang WH, Peng CL, Lin FH, Lin CC. Targeting efficiency and biodistribution of biotinylated-egf-conjugated gelatin nanoparticles administered *via* aerosol delivery in nude mice with lung cancer. *Biomaterials* 2008;**29**:3014–22.
14. Reed MD, Tellez CS, Grimes MJ, Picchi MA, Tessema M, Cheng YS, et al. Aerosolised 5-azacytidine suppresses tumour growth and reprogrammes the epigenome in an orthotopic lung cancer model. *Brit J Cancer* 2013;**109**:1775–81.
15. Taratula O, Kuzmov A, Shah M, Garbuzenko OB, Minko T. Nanostructured lipid carriers as multifunctional nanomedicine platform for pulmonary co-delivery of anticancer drugs and sirna. *J Control Release* 2013;**171**:349–57.
16. Godugu C, Patel AR, Doddapaneni R, Marepally S, Jackson T, Singh M. Inhalation delivery of telmisartan enhances intratumoral distribution of nanoparticles in lung cancer models. *J Control Release* 2013;**172**:86–95.
17. Garbuzenko OB, Saad M, Pozharov VP, Reuhl KR, Mainelis G, Minko T. Inhibition of lung tumor growth by complex pulmonary delivery of drugs with oligonucleotides as suppressors of cellular resistance. *Proc Natl Acad Sci U S A* 2010;**107**:10737–42.
18. Yang MY, Chan JGY, Chan H-K. Pulmonary drug delivery by powder aerosols. *J Control Release* 2014;**193**:228–40.
19. Chow AHL, Tong HHY, Chattopadhyay P, Shekunov BY. Particle engineering for pulmonary drug delivery. *Pharm Res* 2007;**24**:411–34.
20. Lee W-H, Loo C-Y, Traini D, Young PM. Nano- and micro-based inhaled drug delivery systems for targeting alveolar macrophages. *Expert Opin Drug Deliv* 2015;**12**:1009–26.
21. Rawat A, Majumder QH, Ahsan F. Inhalable large porous microspheres of low molecular weight heparin: *in vitro* and *in vivo* evaluation. *J Control Release* 2008;**128**:224–32.
22. Ungaro F, RdEdV Bianca, Giovino C, Miro A, Sorrentino R, Quaglia F, et al. Insulin-loaded PLGA/cyclodextrin large porous particles with improved aerosolization properties: *in vivo* deposition and hypoglycaemic activity after delivery to rat lungs. *J Control Release* 2009;**135**:25–34.
23. Yang Y, Bajaj N, Xu P, Ohn K, Tsifansky MD, Yeo Y. Development of highly porous large PLGA microparticles for pulmonary drug delivery. *Biomaterials* 2009;**30**:1947–53.
24. Zhou GB, Kang H, Wang L, Gao L, Liu P, Xie J, et al. Oridonin, a diterpenoid extracted from medicinal herbs, targets AML1-ETO fusion protein and shows potent antitumor activity with low adverse effects on t(8;21) leukemia *in vitro* and *in vivo*. *Blood* 2006;**109**:3441–50.
25. Zhang Y, Wu Y, Wu D, Tashiro S, Onodera S, Ikejima T. NF- $\kappa$ B facilitates oridonin-induced apoptosis and autophagy in HT1080 cells through a p53-mediated pathway. *Arch Biochem Biophys* 2009;**489**:25–33.
26. Li CY, Wang EQ, Cheng Y, Bao JK. Oridonin: an active diterpenoid targeting cell cycle arrest, apoptotic and autophagic pathways for cancer therapeutics. *Int J Biochem Cell Biol* 2011;**43**:701–4.
27. Kang N, Zhang J-H, Qiu F, Tashiro S-i, Onodera S, Ikejima T. Inhibition of EGFR signaling augments oridonin-induced apoptosis in human laryngeal cancer cells *via* enhancing oxidative stress coincident with activation of both the intrinsic and extrinsic apoptotic pathways. *Cancer Lett* 2010;**294**:147–58.
28. Jiang T, Singh B, Li H-S, Kim Y-K, Kang S-K, Nah J-W, et al. Targeted oral delivery of BMPB vaccine using porous PLGA microparticles coated with M cell homing peptide-coupled chitosan. *Biomaterials* 2014;**35**:2365–73.
29. Fan J-B, Huang C, Jiang L, Wang S. Nanoporous microspheres from controllable synthesis to healthcare applications. *J Mater Chem B* 2013;**1**:2222–35.
30. Ungaro F, Giovino C, Coletta C, Sorrentino R, Miro A, Quaglia F. Engineering gas-foamed large porous particles for efficient local delivery of macromolecules to the lung. *Eur J Pharm Sci* 2010;**41**:60–70.
31. Liu W, Ao L, Zhou Z, Cui Z, Zhou Y, Yuan X, et al. CPG island hypermethylation of multiple tumor suppressor genes associated with loss of their protein expression during rat lung carcinogenesis induced by 3-methylcholanthrene and diethylnitrosamine. *Biochem Biophys Res Commun* 2010;**402**:507–14.
32. Zhou X, Zhang X, Ye Y, Zhang T, Wang H, Ma Z, et al. Nanostructured lipid carriers used for oral delivery of oridonin: an effect of ligand modification on absorption. *Int J Pharm* 2015;**479**:391–8.
33. Patel B, Gupta V, Ahsan F. PEG-PLGA based large porous particles for pulmonary delivery of a highly soluble drug, low molecular weight heparin. *J Control Release* 2012;**162**:310–20.
34. Jia L, Shen J, Zhang D, Duan C, Liu G, Zheng D, et al. *In vitro* and *in vivo* evaluation of oridonin-loaded long circulating nanostructured lipid carrier. *Int J Biol Macromol* 2012;**50**:523–9.
35. Li S, Liu Y, Liu T, Zhao L, Zhao J, Feng N. Development and *in-vivo* assessment of the bioavailability of oridonin solid dispersions by the gas anti-solvent technique. *Int J Pharm* 2011;**411**:172–7.
36. Li C, Zhang D, Guo H, Hao L, Zheng D, Liu G, et al. Preparation and characterization of galactosylated bovine serum albumin nanoparticles for liver-targeted delivery of oridonin. *Int J Pharm* 2013;**448**:79–86.
37. Thomas C, Gupta V, Ahsan F. Particle size influences the immune response produced by hepatitis B vaccine formulated in inhalable particles. *Pharm Res* 2010;**27**:905–19.
38. Papetti M, Herman IM. Mechanisms of normal and tumor-derived angiogenesis. *Am J Physiol Cell Physiol* 2002;**282**:947–70.
39. Li Y, Ahmed F, Ali S, Philip PA, Kucuk O, Sarkar FH. Inactivation of nuclear factor  $\kappa$ B by soy isoflavone genistein contributes to increased apoptosis induced by chemotherapeutic agents in human cancer cells. *Cancer Res* 2005;**65**:6934–42.
40. Matthews GM, Newbold A, Johnstone RW. Intrinsic and extrinsic apoptotic pathway signaling as determinants of histone deacetylase inhibitor antitumor activity. *Adv Cancer Res* 2012;**116**:165–97.
41. Sun J, Li Y, Ding Y, Wang J, Geng J, Yang H, et al. Neuroprotective effects of gallic acid against hypoxia/reoxygenation-induced

- mitochondrial dysfunctions *in vitro* and cerebral ischemia/reperfusion injury *in vivo*. *Brain Res* 2014;**1589**:126–39.
42. Binet MT, Doyle CJ, Williamson JE, Schlegel P. Use of JC-1 to assess mitochondrial membrane potential in sea urchin sperm. *J Exp Mar Biol Ecol* 2014;**452**:91–100.
  43. Jiang J, Li L, Xie M, Fuji R, Liu S, Yin X, et al. SPATA4 counteracts etoposide-induced apoptosis via modulating BCL-2 family proteins in HeLa cells. *Biol Pharm Bull* 2015;**38**:1458–63.
  44. Tian CL, Wen Q, Fan TJ. Cytotoxicity of atropine to human corneal epithelial cells by inducing cell cycle arrest and mitochondrion-dependent apoptosis. *Exp Toxicol Pathol* 2015;**67**:517–24.
  45. Zhao C, Qin G, Gao W, Chen J, Liu H, Xi G, et al. Potent proapoptotic actions of dihydroartemisinin in gemcitabine-resistant a549 cells. *Cell Signal* 2014;**26**:2223–33.
  46. Rahman M, Hasan MR. Cancer metabolism and drug resistance. *Metabolites* 2015;**5**:571–600.